AD NUMBER		
AD829216		
LIMITATION CHANGES		
TO:		
Approved for public release; distribution is unlimited.		
FROM:		
Distribution authorized to U.S. Gov't. agencies and their contractors; Administrative/Operational Use; JUN 1967. Other requests shall be referred to Air Force Space and Missile Systems Organization, SMSD, Los Angeles AFB, CA 90045.		
AUTHORITY		
samso, usaf ltr, 28 feb 1972		

IMR-617

AD829216

INTERNAL MEMORANDUM
RELEASABLE

ANALYSIS OF SMALL PHOTOGRAPHIC IMAGES OF LINE TARGETS

by

H. F. Gilmore

June 1967

STATEMENT

SAMSO / SMSO Los Angeles AFS
CA 90045

*THIS DOCUMENT MAY NOT BE REPRODUCED
WITHOUT PRIOR PERMISSION FROM*

DEFENSE RESEARCH CORPORATION

6300 Hollister Avenue
P.O. BOX 3587 • SANTA BARBARA, CALIFORNIA • 93105

D D C
APR 1 1968
C

ABSTRACT

Using a particular model of the photographic point spread function derived previously, the images which would be expected from a reentry body plus a luminous wake and from a point target moved uniformly during exposure are calculated and compared. The former images exhibit a pronounced head and faint tail which do not appear in the latter.

Two calibration procedures for images of the latter type may be considered, based on the use of either the image growth law for line calibration images or the image growth law for point calibration images. The accuracy of either method depends on the point spread function of the camera. In general the first procedure is accurate for long images but may have a 50% error for images having small length-to-width ratios. The second may have a 30% error for long images but is accurate for short images; it is felt that this procedure will be more satisfactory in practice.

THIS PAGE INTENTIONALLY BLANK

CONTENTS

THIS PAGE INTENTIONALLY BLANK

ILLUSTRATIONS

THIS PAGE INTENTIONALLY BLANK

I.   <u>INTRODUCTION</u>

In the field of reentry measurements, photographic images of line targets--that is, targets which are for practical purposes extended in only one direction--are of considerable importance, since not only do such images constitute the output of ballistic cameras, but they are produced by cine cameras when tracking is imperfect or the reentry body has a wake. When making reentry measurements with cine cameras, it is necessary to distinguish between the latter two types of images, and to have adequate procedures for extracting quantitative data from each.

In this memorandum a consideration of these requirements is based on calculations of the images which would in theory be obtained with given camera point spread functions. The first part compares images which result from uniform rectilinear smearing with the images of reentry bodies with wakes. The second part discusses two calibration procedures for the former images. It will be recognized that in such a treatment many factors such as the Eberhardt effect, reciprocity failure, variation of camera resolution over the image plane, and collimator resolution are neglected. However, the calculations here should be of value in suggesting further experimentation and calculation.

II.   IMAGES OF MOVING TARGETS

We consider a photographic system having a point spread function $C(x,y)$ and a line spread function $A(x)$ with the following usual relations holding:

$$\int\int_{\infty} C(x,y)\ dx\ dy = 1$$

$$\int_{-\infty}^{\infty} C(x,u)\ du = A(x)$$

Consider the target image produced by a moving unresolved point. If the power available from the point is W_p, and it follows the path $x = x(t)$, $y = y(t)$, the energy distribution produced in the emulsion in exposure time Δt starting at time 0 is

$$E_p(x,y) = W_p \int_0^{\Delta t} C[x - x(t),\ y - y(t)]\ dt$$

If $x(t) = 0$, and $y(t) = v\left(t - \frac{\Delta t}{2}\right)$, and $v\Delta t$ is set equal to $2a$ so the geometrical image of the point moves along the y axis from $y = -a$ at time zero to $y = +a$ at time Δt, then

$$E_p(x,y) = W_p \int_0^{\Delta t} C(x, y - vt + a)\ dt$$

Changing variables gives

$$E_p(x,y) = W_p\ \Delta t\ \frac{1}{2a} \int_{y-a}^{y+a} C(x,u)\ du \qquad (1)$$

8

The point spread function of various cameras can be approximated by the function[1]

$$C(x,y) = \frac{A - 1}{\pi} \frac{\varepsilon^{2(A - 1)}}{(\varepsilon^2 + x^2 + y^2)^A} \tag{2}$$

where A and ε are characteristic of the particular camera. The point spread function of the TRAP III High Speed Camera is described by this expression with A = 1.5 and ε = 13 microns. For A = 1.5,

$$E_p(x,y) = \frac{W_p \, \Delta t \, \varepsilon}{4a\pi} \int_{y-a}^{y+a} \frac{du}{(\varepsilon^2 + x^2 + u^2)^{3/2}}$$

$$= \frac{W_p \, \Delta t \, \varepsilon}{4a\pi(\varepsilon^2 + x^2)} \left[\frac{y + a}{\sqrt{\varepsilon^2 + x^2 + (y + a)^2}} - \frac{y - a}{\sqrt{\varepsilon^2 + x^2 + (y - a)^2}} \right]$$

At the center of the image,

$$E_p(0,0) = W_p \, \Delta t \, \frac{1}{2\pi\varepsilon \sqrt{\varepsilon^2 + a^2}}$$

The shape of the image may be described by giving the contour lines along which, for α constant,

$$E_p(x,y) = \alpha E_p(0,0)$$

Contours have been computed for $\alpha = 10^{-2}$ and $\alpha = 10^{-3}$ and three values of a, and the results are shown in Fig. 1.
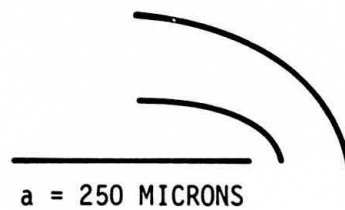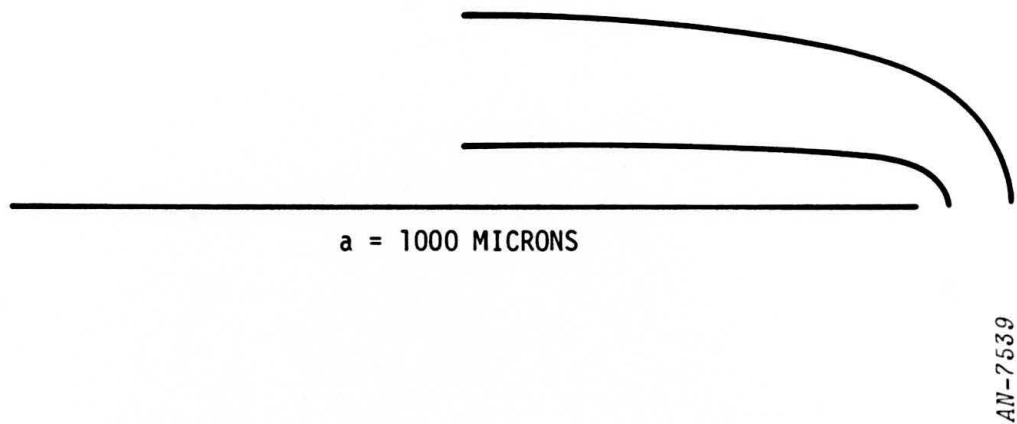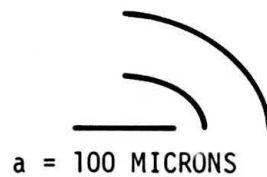
Figure 1.   Equal Intensity Contours for Three Line Targets: Contours Drawn at 10^{-2} and 10^{-3} Times Peak

III. IMAGES EXHIBITING RESOLVED WAKES

Now consider the structure of elongated images when these are not due to image motion during exposure, but rather result from a small body plus a wake. It will be supposed that the geometrical image of the body is a spatial δ-function (a true point) and that the geometrical image of the wake is a single line behind the body. The power per unit length received from the wake will be supposed to be a maximum at the body, and to decrease linearly with distance behind the body until it reaches zero. Thus it is assumed that the body is unresolved, and that the wake is not resolved in width, but is resolved in length.

The energy distribution in the image plane of the optical system can be obtained by adding the energy distribution due to the body to that due to the wake, so these distributions may be considered separately. Also, since the exposure time, Δt, is not of interest here, it may be assumed that $\Delta t = 1$. Then if the power received from the body is W_b and the optical point spread function is $C(x,y)$, the energy distribution in the image of the body alone, I_b, would be simply

$$I_b = W_b C(x,y)$$

The assumption about the wake given above requires that the geometrical image of the wake have the form

$$f(x,y) = W_\omega (1 + \frac{y}{d}) \, \delta(x)$$

for $0 \geq y \geq -d$. This represents a wake extending a distance d along the negative y axis from a body assumed to be at the origin; W_ω is the power per unit length at the head of the wake. The total power from the wake is thus

$$\int_{-\infty}^{\infty} \int_{-d}^{0} W_\omega (1 + \frac{y}{d}) \, \delta(x) \, dy \, dx = \frac{W_\omega}{d} \int_{-d}^{0} (d + y) dy = \frac{W_\omega d}{2}$$

The energy distribution in the image of the wake alone is

$$I_\omega(x,y) = \int\limits_{\eta=y}^{y+d} \int\limits_{-\infty}^{\infty} C(\xi,\eta) \; W_\omega(1 + \frac{y - \eta}{d}) \; \delta(x - \xi)d\xi \; d\eta$$

$$= \int\limits_{\eta=y}^{y+d} C(x,\eta) \; W_\omega(1 + \frac{y - \eta}{d}) \; d\eta$$

or

$$I_\omega(x,y) = \frac{W_\omega}{d} \int\limits_0^d uC(x,d + y - u) \; du$$

It will now be assumed as before that the point spread function in question is

$$C(x,y) = \frac{\epsilon}{2\pi} \; \frac{1}{(\epsilon^2 + x^2 + y^2)^{3/2}}$$

With this expression the image of the body alone has the form

$$I_b(x,y) = \frac{\epsilon W_b}{2\pi} \; \frac{1}{\left[\epsilon^2 + x^2 + y^2\right]^{3/2}}$$

and the image of the wake alone is given by

$$I_\omega(x,y) = \frac{W_\omega \epsilon}{2\pi d} \int\limits_0^d \frac{u \; du}{\left[\epsilon^2 + x^2 + (d + y - u)^2\right]^{3/2}}$$

From the indefinite integral

$$\int \frac{x\,dx}{\left[a + bx + cx^2\right]^{3/2}} = -\frac{1}{c\sqrt{a + bx + cx^2}}\left[1 + \frac{b(2cx + b)}{4ac - b^2}\right]$$

we obtain

$$I_\omega(x,y) = \frac{W_\omega \epsilon}{2\pi d(\epsilon^2 + x^2)}\left\{\left[\epsilon^2 + x^2 + (d + y)^2\right]^{1/2} - \frac{\epsilon^2 + x^2 + y^2 + dy}{\left[\epsilon^2 + x^2 + y^2\right]^{1/2}}\right\}$$

The energy density in the overall image is, of course,

$$I_b(x,y) + I_\omega(x,y)$$

To afford an insight into the appearance of the image of the body and wake, a particular example has been considered. It was supposed that ϵ = 12.5 microns (more convenient for calculation than the 13 microns determined for the high speed camera), that d, the length of the geometrical image of the wake, was 1000 microns, and that the total energy received from the body was ten times that received from the wake. Thus

$$10\left(\frac{W_\omega d}{2}\right) = W_b$$

$$W_\omega = 2 \times 10^{-4}\, W_b$$

and the energy density at the origin is obtained from

$$I_b(0,0) + I_\omega(0,0) = \frac{W_b}{2\pi\epsilon^2} + \frac{W_\omega}{2\pi d\epsilon}\left[\left(\epsilon^2 + d^2\right)^{1/2} - \epsilon\right]$$

Contour maps have been plotted for the body alone, the wake alone, and the body plus wake (Figs. 2, 3, and 4). In each case the four contours pass through points where I_b, I_ω, or $I_b + I_\omega$ is a given fraction times the intensity at the origin, $I_b(0,0) + I_\omega(0,0)$. The contours can be considered to be the edges of the images which would be seen as the power received from the target increased by multiples of 10 from a level sufficient to carry the emulsion well into saturation at the center of the geometrical image of the body.

It will be noted that the body plus wake images differ significantly from the wake images, or from those due to uniform motion, in having a definite well-defined head followed by a much fainter tail. The images shown look much like actual resolved images of large reentry bodies with wakes.

IV. CALIBRATION AND DATA REDUCTION PROCEDURES

We now consider two techniques for the reduction of data from integrating cameras when images are blurred through uniform rectilinear motion of the image during exposure. The methods discussed apply to both saturated and unsaturated images, but are especially valuable for the former. The first procedure consists of the following four steps:

1. Obtain the usual point-source image-growth-law calibration curve giving image diameter versus irradiance with a small source aperture in the collimator. (This will be necessary in general for the measurement of unsmeared target images.)

2. Measure the width $2x_1$ and the length $2y_1$ of the elongated image at the same fixed density level used in deriving the above calibration curve.

3. Use $2x_1$ and the calibration curve to obtain an initial approximation to the target irradiance.

4. Multiply this initial approximation by the ratio y_1/x_1 to obtain the final approximation to target irradiance.

The second calibration procedure which has been investigated is based on the use of a slit source aperture in the collimator. This procedure is as follows:

S1. Obtain a second image-growth-law calibration curve giving line image width versus irradiance (per unit image length) with a slit source aperture in the collimator.

S2. Measure the width $2x_1$ and the length $2y_1$ of the elongated target image at the same fixed density level used in deriving this calibration curve.

S3. Use $2x_1$ and the calibration curve to obtain an approximation to the target irradiance per unit length.

S4. Multiply this approximation by $2y_1$ to obtain a final approximation to target irradiance.

A. ANALYSIS OF FIRST CALIBRATION PROCEDURE

Suppose that we have a photographic system having a circularly symmetrical point spread function $C(x,y)$. Calibration images are made with an unresolved point source, and the diameters, $2r_c$, of these images are measured at a fixed threshold level E_t. Since the energy distribution, $E_c(x,y)$, in the calibration images due to such a source which is providing power W_c during exposure time Δt is

$$E_c(x,y) = W_c \Delta t \ C(x,y)$$

the relationship between W_c and r_c can be obtained from

$$E_t = W_c \Delta t \ C(r_c,0)$$

and hence is

$$W_c = \frac{E_t}{\Delta t \ C(r_c,0)} \tag{3}$$

This is the system image growth law, which is thus proportional to the reciprocal of the point spread function.

For the elongated target images, x_1 and y_1 can be calculated from Eq. (1):

$$E_t = E_p(x_1,0) = W_p \Delta t \ \frac{1}{2a} \int_{-a}^{a} C(x_1,u) \ du \tag{4}$$

$$E_t = E_p(0,y_1) = W_p \ t \ \frac{1}{2a} \int_{y_1-a}^{y_1+a} C(0,u) \ du \tag{5}$$

Also, letting α be the ratio between E_t and the energy density in the center of the image,

$$E_t = \alpha \; W_p \Delta t \; \frac{1}{2a} \int_{-a}^{a} C(0,u) \; du \qquad (6)$$

The suggested procedure requires that $2x_1$ and $2y_1$ be measured, a corresponding W_c be determined by substituting x_1 for r_c in Eq. (3), and this value of W_c be multiplied by y_1/x_1 to obtain a final computed value of target power. Denoting the computed value of target power by $\left| W_p \right|_{comp}$ we have, using Eqs. (3) and (4)

$$\left| W_p \right|_{comp} = \frac{y_1}{x_1} \; \frac{E_t}{\Delta t \; C(x_1,0)}$$

or

$$\frac{\left| W_p \right|_{comp}}{W_p} = \frac{y_1}{x_1} \; \frac{1}{2a} \; \frac{\displaystyle\int_{-a}^{a} C(x_1,u) \; du}{C(x_1,0)} \qquad (7)$$

where y_1 and x_1 are to be obtained from Eqs. (4) and (5).

It will be observed upon inspection of Eqs. (4) through (7) that in addition to a and the form of $C(x,y)$, either E_t or α must be specified in order to calculate the relative error. For saturated images α may in practice be between 10^{-2} and perhaps 10^{-5}; the exact value is not expected to produce a great effect in the nature of the calculated results. In this memorandum only one or two values of α have been selected for each a and $C(x,y)$ in order to reduce the computation time required. With this limitation, the accuracy of the proposed calibration method has been evaluated for three point spread functions having the form given by Eq. (2), with values of 1.5, 2, and 2.5 for A; these cover the range of image growth laws encountered so far. The calculated values of the relative accuracy are shown in Fig. 5 for various choices of the parameters.
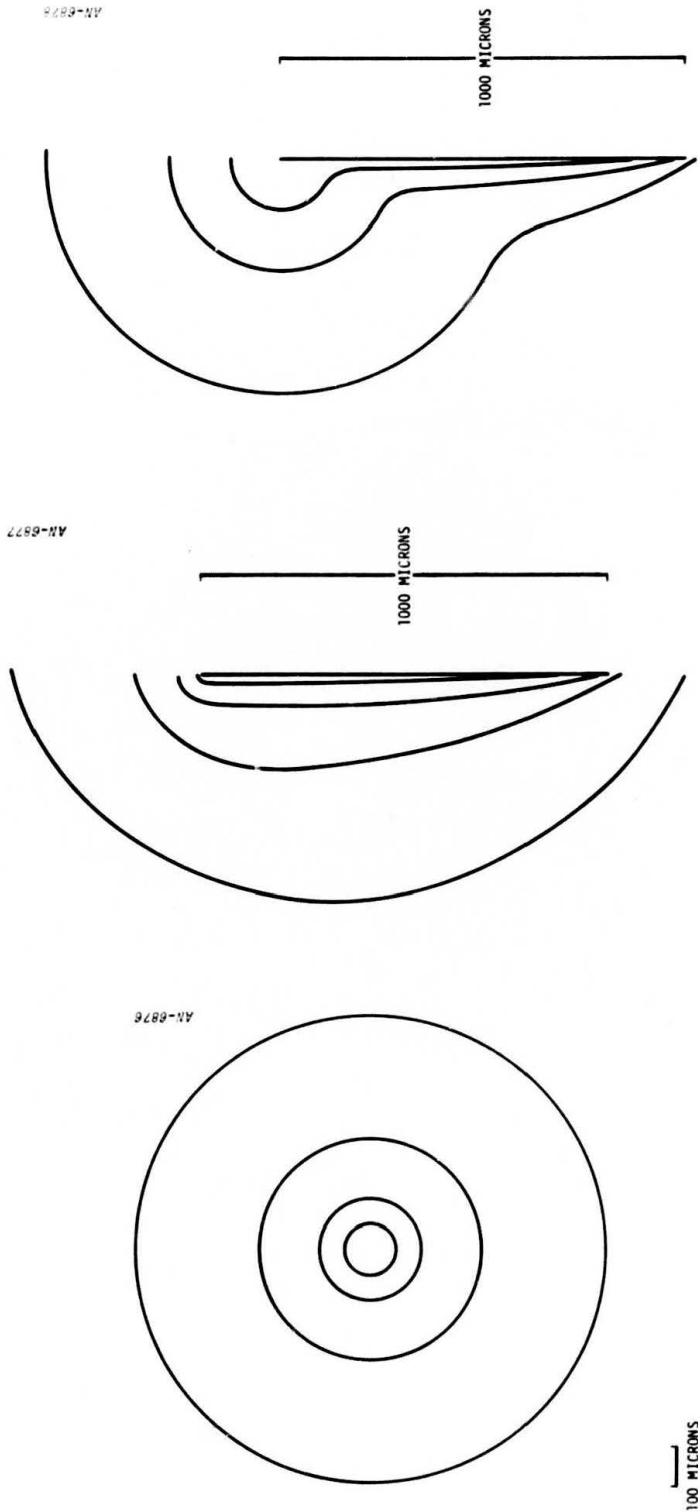
Figure 4.

Equal Intensity Contours
for Point Target (Fig. 2)
Plus Hypothetical Wake
(Fig. 3): Contours
Drawn at 10^{-3}, 10^{-4}, 10^{-5}
Times Peak.

Figure 3.

Equal Intensity Contours
for Hypothetical Wake.
Total Wake Energy 0.1
Times Total Energy of
Point Target of Fig. 2.
Contours Drawn at 10^{-3},
10^{-4}, 10^{-5}, and 10^{-6}
Times Peak of Fig. 2.

Figure 2.

Equal Intensity Contours
for Point Target: Contours
Drawn at 10^{-2}, 10^{-3}, 10^{-4},
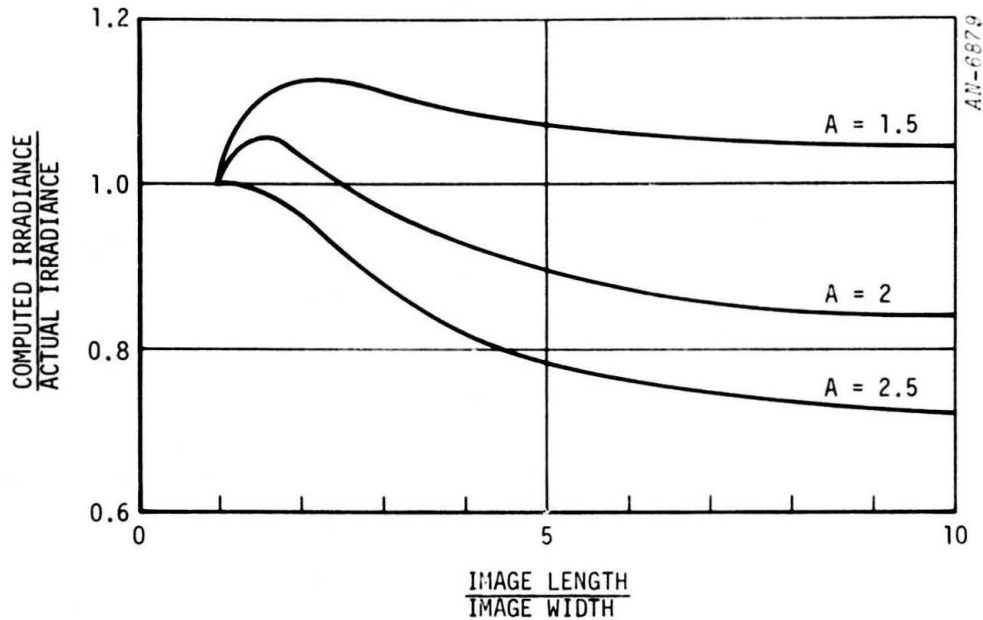and 10^{-5} Times Peak.

Figure 5. Ratio of Computed Irradiance to Actual Irradiance as a Function of the Length-to-Width Ratio of Smeared Images for First Calibration Procedure. (A is One-Half the Limiting Slope of the Image Growth Law on a Log-Log Plot.)

It can be seen that the proposed procedure is fairly accurate for images which are only slightly elongated, but may introduce an error as great as 33% for very long images. This is considered satisfactory, since in practice the images to be measured are generally not very long, and errors of this magnitude are usually acceptable.

B.   ANALYSIS OF SECOND CALIBRATION PROCEDURE

The alternate calibration method considered for such targets is based on using a slit source in the collimator. If the power per unit length in the geometrical image of the slit is W_s, the exposure time is Δt, and the geometrical image of the slit coincides with the y axis, the energy distribution per unit length in the calibration image is

$$E_s(x,y) = W_s \Delta t \int_{-\infty}^{\infty} C(x,y)\ dy = W_s \Delta t\ A(x)$$

where $A(x)$ is the system line spread function. If a series of such images is made with different values of W_s and the half-width x_s of each image is measured at a fixed level E_t, the resulting image growth law is obtained from

$$E_t = W_s \Delta t \int_{-\infty}^{\infty} C(x_s, y) \, dy$$

and hence is

$$W_s = \frac{E_t}{\Delta t \int_{-\infty}^{\infty} C(x_s, y) \, dy} \tag{8}$$

In order to determine W_p responsible for an image of the form given by Eq. (1), some estimate of the effective image length must be obtained from the image. If this estimate is denoted by $2 \, \tilde{a}$, the computed value of W_p, $\left[W_p\right]_{\text{comp } 2}$, is

$$\left[W_p\right]_{\text{comp } 2} = 2 \, \tilde{a} \, W_s$$

Hence, using Eqs. (4) and (8),

$$\frac{\left[W_p\right]_{\text{comp } 2}}{W_p} = \frac{2 \, \tilde{a} \, W_s}{W_p} = \frac{\dfrac{\tilde{a}}{a} \int_{-a}^{a} C(x_1, y) \, dy}{\int_{-\infty}^{\infty} C(x_1, y) \, dy}$$

The only reasonable choice for $\tilde{a}$ appears to be $\tilde{a} = y_1$ where y_1 satisfies Eq. (5). The choice $\tilde{a} = y_1 - x_1$ which might be considered leads to the unsatisfactory result

$$\lim_{a \to 0} \frac{\left[W_p\right]_{\text{comp } 2}}{W_p} = 0$$

With $\tilde{a} = y_1$ we have

$$\frac{\left[W_p\right]_{comp\ 2}}{W_p} = 2y_1 \frac{\frac{1}{2a} \int_{-a}^{a} C(x_1,y)\ dy}{\int_{-\infty}^{\infty} C(x_1,y)\ dy} \tag{9}$$

We note that as a increases

$$\underset{a\to\infty}{Lim} \frac{\left[W_p\right]_{comp\ 2}}{W_p} = 1$$

and as a decreases

$$\underset{a\to 0}{Lim} \frac{\left[W_p\right]_{comp\ 2}}{W_p} = \frac{2y_1\ C(x_1,0)}{\int_{-\infty}^{\infty} C(x_1,y)\ dy}$$

Comparing Eq. (9) with Eq. (7), we obtain

$$\frac{\left[W_p\right]_{comp\ 2}}{W_p} = \left\{\frac{\left[W_p\right]_{comp}}{W_p}\right\}\left\{\frac{2x_1\ C(x_1,0)}{\int_{-\infty}^{\infty} C(x_1,y)\ dy}\right\}$$

When $C(x,y) = \frac{A-1}{\pi} \frac{\varepsilon^{2(A-1)}}{(\varepsilon^2 + x^2 + y^2)^A}$ it is found that

$$\int_{-\infty}^{\infty} C(x,y)\ dy = \frac{\Gamma(1/2)\Gamma(A-1/2)}{\Gamma(A)} \cdot \frac{A-1}{\pi} \frac{\varepsilon^{2(A-1)}}{\left[\varepsilon^2 + x^2\right]^{A-1/2}}$$

and hence

$$\frac{\left[W_p\right]_{comp\ 2}}{W_p} = \left\{\frac{\left[W_p\right]_{comp}}{W_p}\right\} \left\{\frac{2\Gamma(A)}{\Gamma(1/2)\Gamma(A-1/2)}\right\} \left\{\frac{x_1}{\left[\epsilon^2 + x_1^2\right]^{1/2}}\right\}$$

This enables the relative error for calibration with a slit source to be obtained from the calculations which gave Fig. 5; the results for the three values of A considered are shown in Fig. 6.

Again, the accuracy of this procedure depends on the system image growth law. It will be noted that this procedure gives the correct irradiance for large values of the ratio y_1/x_1, but is not as accurate when y_1/x_1 is close to unity. This procedure is considered inferior to the previous one because most elongated images are relatively short and thus
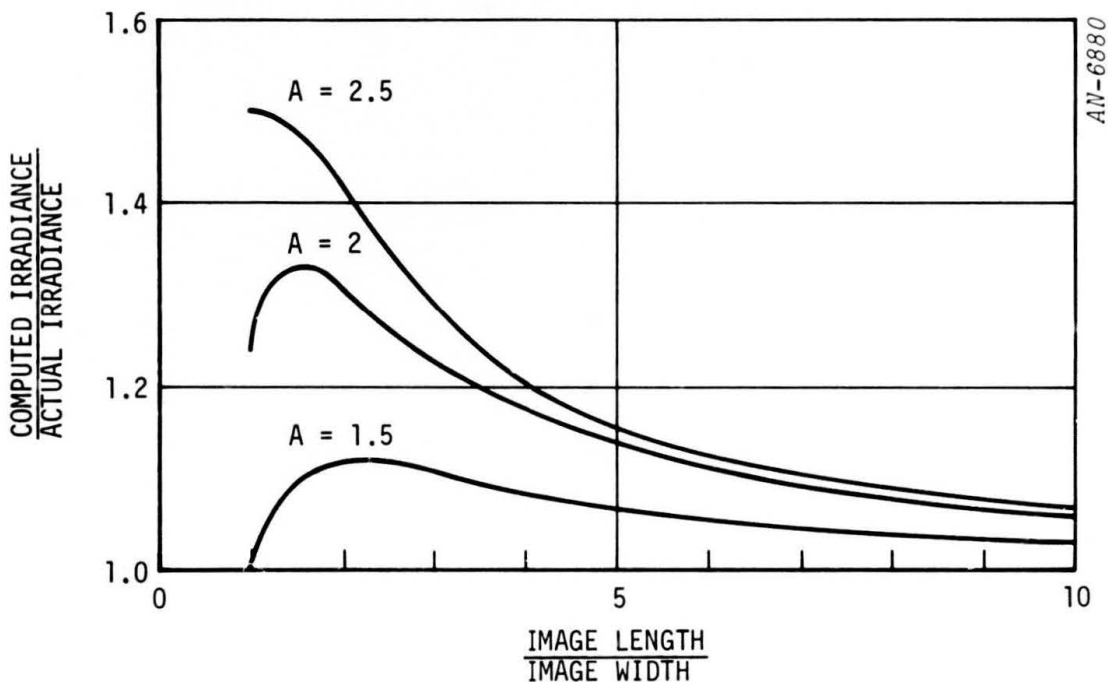

Figure 6. Ratio of Computed Irradiance to Actual Irradiance as a Function of the Length-to-Width Ratio of Smeared Images for Calibration with Slit. (A is One-Half the Limiting Slope of the Image Growth Law on a Log-Log Plot.)

fall in the region where the previous method is more accurate, and because the second method requires an additional set of calibration measurements while the first makes use of the standard calibration curve needed for data reduction of unsmeared targets.

THIS PAGE INTENTIONALLY BLANK

REFERENCE

1.   H. F. Gilmore, <u>The Use of Image Growth Laws in Analyzing Reentry Measurement Cameras,</u> Defense Research Corporation TM 462, August 1966 (UNCLASSIFIED).

THIS PAGE INTENTIONALLY BLANK